Bull. Mater. Sci., Vol. 36, No. 3, June 2013, pp. 411–416. © Indian Academy of Sciences.

Effect of Zn doping on optical properties and photoconductivity of SnS_2 nanocrystalline thin films

R ETEFAGH[1], N SHAHTAHMASEBI[2] and M KARIMIPOUR[3,*]
[1]Payame Nour University, Mashhad, Iran
[2]Nano Research Centre, Ferdowsi University, Mashhad, Iran
[3]Department of Physics, Faculty of Science, Vali-e-Asr Rafsanjan University, Rafsanjan, Iran

MS received 20 April 2012; revised 19 June 2012

Abstract. **Zn-doped SnS_2 thin films have been deposited simply by spray pyrolysis technique. The doping level was changed from [Zn/Sn] = 0 to 7·5 at%. The films were characterized by means of X-ray diffraction, scanning tunneling microscopy (STM), energy dispersive X-ray analysis (EDX), photoluminescence and UV-Vis spectroscopy. XRD patterns of the films with different zinc contents show that all samples have polycrystalline structure with Berndtite dominant phase and preferred orientation of (001) growth plane. Zn insertion causes a significant decrease in grain size. Optical bandgap of the films have been calculated for different dopant concentrations and they lie in the region of 2·3–2·7 eV. Surprisingly, regardless of doping level, the luminescent properties of films are related to the fundamental bandgap energy and deep levels inside the bandgap. Photoconductivity of the films have been measured under visible light. Sensitivity to the light increases by zinc incorporation, which was a large amount for SnS_2:Zn of 7·5%.**

Keywords. **Thin film; spray pyrolysis; tin sulfide; optical properties; photoluminescence; photoconductivity.**

1. Introduction

The current investigations in the field of photovoltaic cells have focused towards the development of low cost and non-toxic materials with simple fabrication methods. According to worldwide researches, among different compounds with possible photovoltaic applications, sulfur salts appear to be the promising candidates (Dittrich *et al* 1995; Koteeswara Reddy and Ramakrishna Reddy 1998, 2006). SnS_2 as a member of compounds with CdI_2 structure, has interesting properties such as high optical absorption coefficient ($>10^4$ cm^{-1}) in the visible range, wide optical bandgap of about 2·5 eV, *n*-type electrical conduction and high photo-conducting behaviour (Thangaraju and Kaliannan 2000). These properties suggest that SnS_2 is an appropriate material for solar cell and opto-electronic device applications (Jiang *et al* 1998). Moreover, excellent sensors for NH_3, H_2S can be fabricated from non-porous Sn_xS_y (Panda *et al* 2007). Doping in semiconductor material can improve its semiconducting properties. Therefore, it is necessary to study doped-Sn_xS_y thin films for various applications. It was reported by Yongli and Shuying (2008) that Ag-doped Sn_xS_y thin films could improve the properties of *p*-type Sn_xS_y thin films, which is necessary for the films used as absorbing materials in solar cells. In work reported by Yan-hui *et al* (2007) that since the pure Sn_xS_y films do not possess appropriate conductivity for solar cells, indium chloride was utilized as a dopant source to the solution for deposition of Sn_xS_y:In films. Various techniques have been used such as atmospheric pressure chemical vapour deposition (APCVD) (Price *et al* 1999), successive ionic layer adsorption and reaction (SILAR) (Sankapal *et al* 2000), chemical solution deposition (Engelken *et al* 1987; Lokhande 1990), vacuum evaporation (George and Joseph 1982; Kawano *et al* 1989), chemical vapour transport (Matsumoto and Tagaki 1983) and dip coating (Ray *et al* 1999).

In this work, the Zn-doped SnS_2 thin films were deposited by spray pyrolysis technique and its optical, structural and photoconductivity properties are studied using X-ray diffraction (XRD), scanning tunneling microscopy (STM), EDX analysis, photoluminescence (PL) and UV-Vis absorption spectroscopy.

2. Experimental

2.1 *Preparation of precursor solution*

The zinc-doped SnS_2 thin films have been deposited on the glass substrates using a typical spray pyrolysis at T_s = 360 °C. The spray deposition parameters such as solution flow rate, nozzle to substrate distance and carrier gas flow rate were kept constant under conditions;

*Author for correspondence (m.karimipour@vru.ac.ir)

10 ml/min, 34 cm and 2·7 atm, respectively. The precursor solution was prepared using (0·02 M) of stannic chloride ($SnCl_4$:$5H_2O$) *n*,*n*-dimethyl thiourea (H_2NCSN_2H) and zinc acetate $(CH_3COO)_2Zn{\cdot}2H_2O$ was dissolved in a mixture of isopropyl alcohol and deionized water with the volumetric ratio of 3:1. Molar ratio of S/Sn was 3:1 and dopant concentration varied from 0 to 7·5 at% (Bagheri Mohagheghi *et al* 2009).

2.2 *Characterization*

X-ray diffraction (XRD) patterns of SnS_2 films were recorded by D8-Advance Bruker system using CuKα (λ = 0·154056 nm) radiation with 2θ in the range 10–70°. The lateral morphology and roughness of the films were studied by means of scanning tunneling microscopy (STM) SS1 system. The optical absorption and transparency as well as luminescence study of films were performed in the wavelength range of 200–1000 nm using Agilent 8453 UV–Vis spectrophotometer and Perkin–Elmer Ls45 flourescence spectrometer, respectively at room temperature.

3. Results and discussion

3.1 *Structural properties*

In figure 1, XRD patterns of the films with different zinc contents show that all samples have polycrystalline structure with Berndtite dominant phase. It also shows that (001) is the main preferential crystalline growth plane. Other Bragg peaks are so weak and are depicted (figure 1, inset) in logarithmic scale for clarity. It shows that with increasing Zn content up to 7·5%, these peaks diminish as well as intensity drop of (001) plane peak due to structural tension. Mean crystallite size subtracted from Scherrer equation

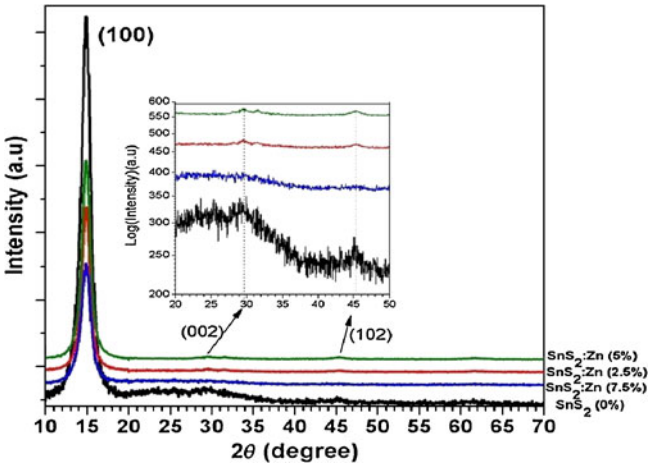

Figure 1. XRD patterns of SnS_2:Zn thin films at different zinc contents.

Table 1. X-ray diffraction data for films (*d*: atomic plane distance, θ: Bragg angle and FWHM: full width at half maximum).

Sample	2θ (degree)	*d* (Å)	FWHM (°)	Mean crystallite size (nm)
Undoped-SnS_2	11·52	5·93	1·35	7
SnS_2:Zn (2·5%)	12·04	5·97	1·10	8
SnS_2:Zn (5%)	11·24	5·96	1·18	8

(Koteeswara Reddy and Ramakrishna Reddy 2005) has been tabulated in table 1. The sizes range from 7 to 8 nm for different Zn concentrations in the films. XRD parameters of the samples show the effect of both uniform and non-uniform strain in the structure of the films. But, the change in the values is not significant and one can be drawn into a conclusion that the films are well crystalline with major (001) growth plane.

For qualitative analysis of chemical composition of the films, EDX analysis of the pure and 7·5 at% doped samples were carried out (figure 2). The results apparently verify Zn atoms as well as S incorporation in the films (see figure 2b).

STM images of 0, 2·5, 5 and 7·5 at% Zn-doped SnS_2 films are demonstrated in figure 3. In undoped SnS_2 film, grains with 87 nm size are observable. An increase in dopant content up to 7·5 at% results in a decrease in grain size up to 9 nm. It shows that the contribution of Zn atoms in the structure of films gives rise to a decrease in size and modification of surface grains. One can say that Zn does not create any order in the films but causes precipitation of S atoms around Sn or Zn ions and concomitantly decreasing the size of grains.

3.2 *Optical properties*

The absorption coefficient (α) of the films is also evaluated from (1), where *t* and *A* are the thickness and absorption of the films, respectively. In order to determine the absorption coefficient and find extinction coefficient, the thickness of the layers (*t*) was obtained by PUMA software. Results show that the thickness of the samples for SnS_2 thin films is roughly 350 nm for all the samples.

The spectral behaviour of the absorption coefficient as a function of energy, $h\nu$, is shown in figure 4.

$$\alpha = 2{\cdot}33A/t. \tag{1}$$

The films have highest absorption coefficient of $\geq 10^4$ cm^{-1}. The absorption coefficient of the films with impure Zn is higher than that of the pure film. The energy bandgap of the films was evaluated using (2):

$$(\alpha h\nu)^2 = A(h\nu - E_g), \tag{2}$$

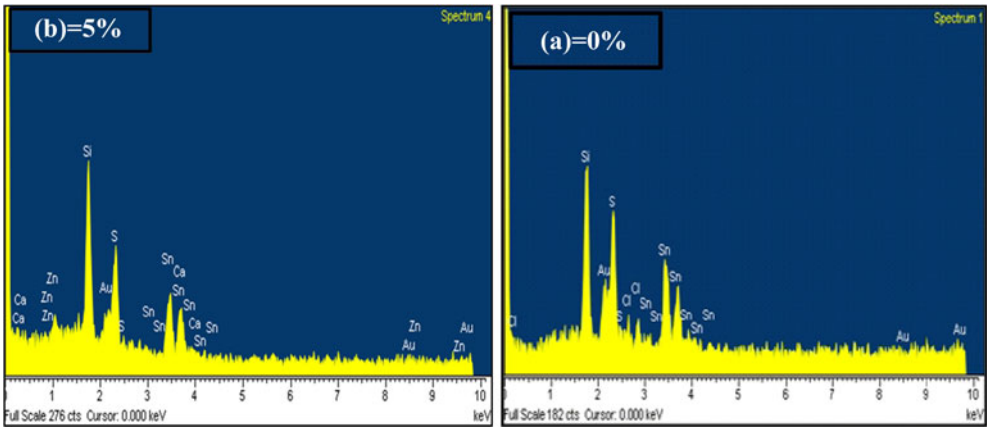

Figure 2. Energy dispersive spectrum of SnS_2:Zn films: (**a**) pure and (**b**) 7·5% Zn-doped. They clearly show presence of S and Zn atoms in structures of films.

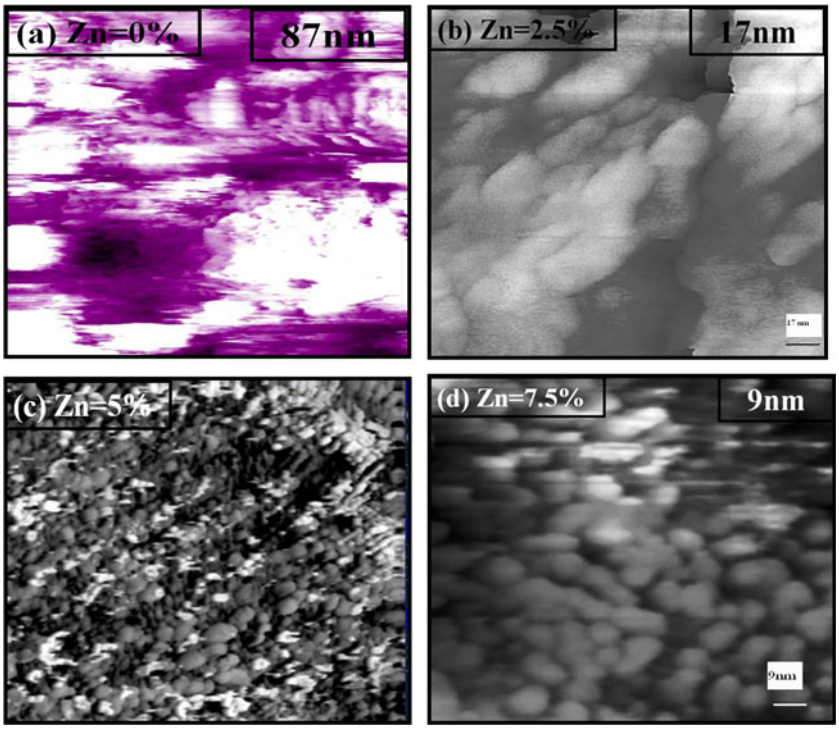

Figure 3. STM photographs of SnS_2:Zn films at different Zn concentrations: (**a**) 0%, (**b**) 2·5%, (**c**) 5% and (**d**) 7·5%.

where α is the absorption coefficient, A the constant and E_g the direct bandgap of the material (Nadeem and Ahmed 2000). The $(\alpha h\nu)^2$ vs photon energy ($h\nu$) plots for SnS_2, SnS_2:Zn films are shown in figure 5 and the calculated energy bandgaps are given in table 2. The plots were linear and indicate a direct optical transition. The optical bandgap is about 2·7 eV in pure SnS_2, which is more than the reported value by Ray and Karanjai (1999). Figure 5 shows that insertion of Zn causes a decrease in energy bandgap. Zn atoms as acceptors create acceptor levels near the edge of conduction band, resulting in a decrease in the bandgap. Precipitation of S around metallic ions creates local states and tails near the edge of conduction band giving rise to decrease in bandgap as well (Koteeswara Reddy and Ramakrishna Reddy 2005).

Photoluminescence spectra of the films are depicted in figure 6. It shows that luminescence of films is independent

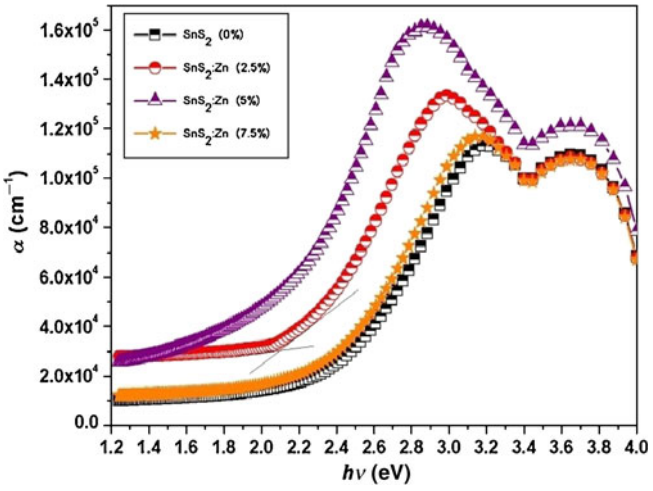

Figure 4. Absorption coefficient vs photon energy of SnS_2:Zn films at different Zn contents. It shows Zn incorporation results and in an increase in film's absorption.

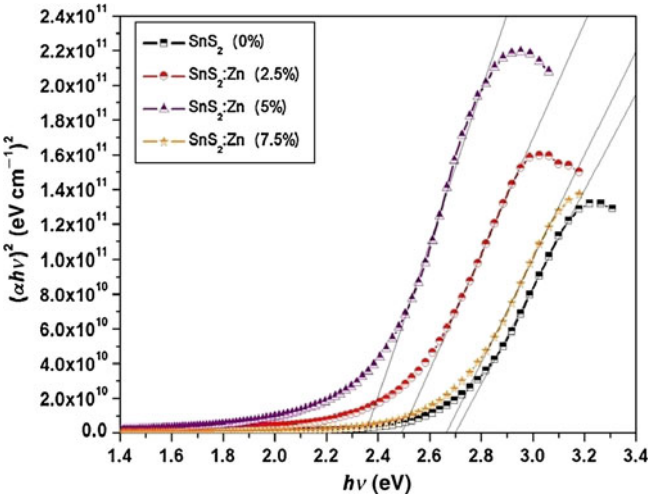

Figure 5. Tauc plot of direct absorption as a function of $h\nu$ for films.

of Zn dopant. The peak corresponding to 2·57 eV shows the fundamental absorption edge for SnS_2 structure. The peak related to the energy of 2·27 eV shows intrinsic local states within the gap. The mentioned states can be caused by non-equivalent number of S atoms in the unit cell of SnS_2 structure. The bandgap of 5% Zn-doped film is about 2·35 eV which has been roughly obtained from PL spectra. The absence of the peak at 2·57 eV can be due to the formation of a tail near the band edge giving rise to the formation of continuous states up to 0·3 eV below band edge. This continuous tail can result in a decrease in carrier life-time concomitant with broadening of emission spectra (Deshpande *et al* 2007; Devika *et al* 2010).

3.3 *Photoconductivity measurements*

The photosensitivity of the films is defined in the following equation:

$$S = (R - R_0)/R_0. \tag{3}$$

R and R_0 are the electrical resistance under light illumination and in the dark resistance, respectively (Sajeesh *et al* 2010). In figure 7, variation of $(R - R_0)/R_0$ vs time is plotted for different dopant Zn-concentrations under variable illumination. If the energy of the illuminated photon is equal or higher than the bandgap energy, it creates the electron–hole pair, therefore, the samples show high conductance. The sensitivity to light increases by zinc incorporation, which is the most at 7·5%, therefore, it is an excellent choice for solar cells application.

Table 2. Optical bandgap of SnS_2 and SnS_2:Zn films calculated from Tauc plot of absorption.

Sample	E_g (eV)
Undoped-SnS_2	2·7
SnS_2:Zn 2·5%	2·5
SnS_2:Zn 5%	2·3
SnS_2:Zn 7·5%	2·6

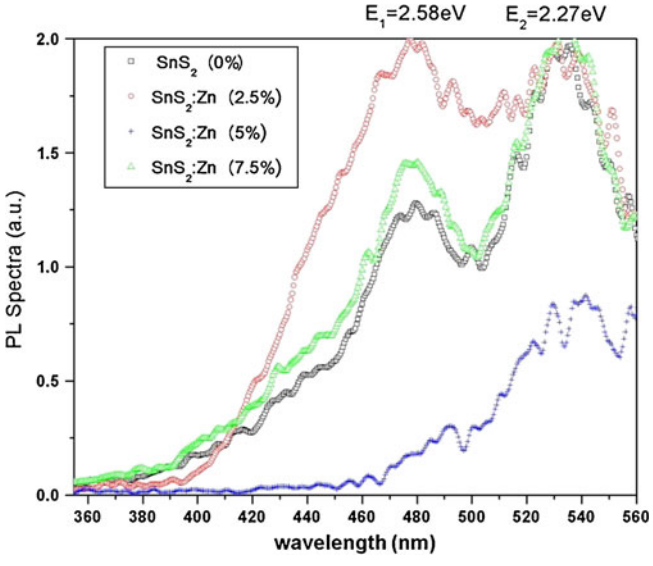

Figure 6. Photoluminescence spectra vs photon energy for SnS_2:Zn and SnS_2 films. It shows excitonic centres of film structure regardless of Zn concentrations which are related to structural defects.

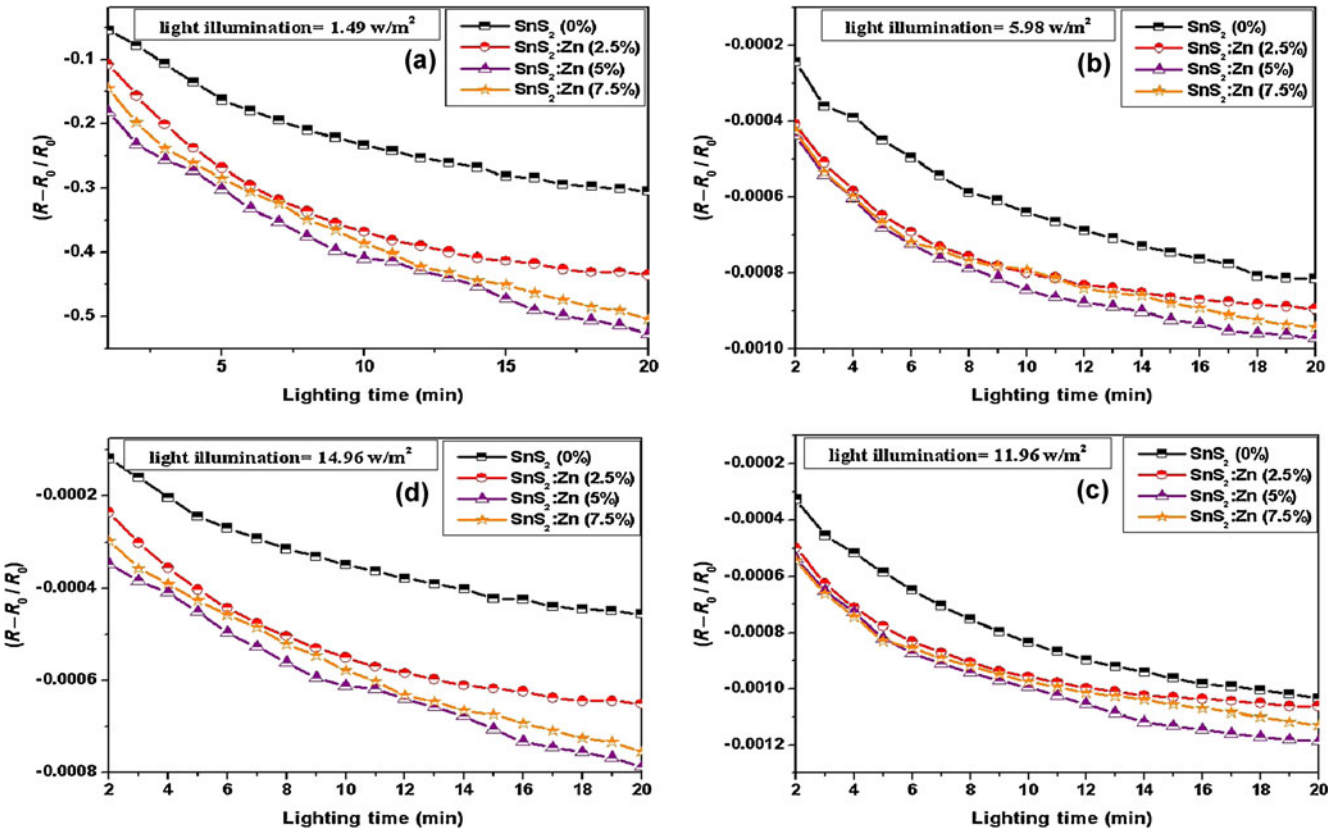

Figure 7. Photoconductivity variation vs irradiated time of films with different Zn concentrations under different illumination powers: (**a**) 1·49 w/m^2, (**b**) 5·98 w/m^2, (**c**) 11·96 w/m^2 and (**d**) 14·96 w/m^2.

4. Conclusions

Nanocrystalline Zn-doped SnS_2 thin films on glass substrate were deposited at 360 °C successfully using simply the spray pyrolysis technique. XRD images show that films are polycrystalline structures with grain size up to 8 nm. The STM image shows contribution of Zn atoms in the structure of films giving rise to a decrease in size and modification of surface grains. In optical characterization of the films shows highest absorption coefficient of $\geq 10^4$ cm^{-1}. The optical bandgap in pure SnS_2 is about 2·7 eV, with increasing impurity, the optical bandgap decreases to 2·3 eV. Photoluminescence properties of SnS_2 on glass were investigated. PL showed two emission peaks at 2·57 and 2·27 eV corresponding to fundamental absorption edge peak and intrinsic local states within the gap, respectively. The sensitivity of layers to the visible light indicates an increase by zinc incorporation. After studying the structural, optical and photoconductivity properties of SnS_2 thin films, the films can be suitably employed in photovoltaic application, for further study.

References

Bagheri Mohagheghi M-M, Shahtahmasebi N, Alinejad M R, Youssefi A and Shokoohi-Saremi M 2009 *J. Solid State Sci.* **11** 233

Deshpande N G, Sagade A A, Gudagea Y G, Lokhande C D and Sharma R 2007 *J. Alloys Compd.* **436** 421

Devika M, Koteeswara Reddy N, Prashantha M, Ramesh K, Venkatramana Reddy S, Hahn Y B and Gunasekhar K R 2010 *Phys. Status Solidi A* **207** 1864

Dittrich H, Vaughan D J, Pattrick R A D, Graeser S, Lux-Steiner M, Kunst R and Lincot D 1995 in *Proceeding of the 13th European phot. solar energy conference*, *Nice, France*, p. 1299

Engelken R D, McClaud H E, Lee C, Slayton M and Ghoreishi H 1987 *J. Electrochem.* **134** 2696

George J and Joseph K S 1982 *J. Appl. Phys.* **15** 1109

Jiang T, Ozine G A O, Verma A and Bedard R L 1998 *J. Mater. Chem.* **8** 1649

Kawano K, Nakata R and Sumita M 1989 *J. Appl. Phys.* **22** 136

Koteeswara Reddy N and Ramakrishna Reddy K T 1998 *Thin Solid Films* **325** 4

Koteeswara Reddy N and Ramakrishna Reddy K T 2005 *Physica B* **368** 25

Koteeswara Reddy N and Ramakrishna Reddy K T 2006 *J. Mater. Res. Bull.* **41** 414

Lokhande C D 1990 *J. Appl. Phys.* **23** 1703

Matsumoto K and Tagaki K 1983 *J. Cryst. Growth* **63** 202

Nadeem M Y and Ahmed W 2000 *Turk. J. Phys.* **24** 651

Panda S K, Antonakos A, Liarokapis E, Bhattacharya S and Chaudhuri S 2007 *J. Mater. Res.* **42** 576

Price L S, Parkin I P, Hardy A M E and Clark R J H 1999 *J. Chem. Mater.* **11** 1792

Ray S C, Karanjai M K and Das Gupta D 1999 *Thin Solid Films* **350** 72

Sajeesh T H, Warrier A R, Sudha Kartha C and Vijayakumar K P 2010 *Thin Solid Films* **518** 4370

Sankapal B R, Mane R S and Lokhande C D 2000 *J. Mater. Res. Bull.* **35** 2027

Sekhar C Ray and Malay K Karanjai 1999 *Thin Solid Films* **350** 72

Thangaraju B and Kaliannan P 2000 *J. Appl. Phys.* **33** 1054

Yan-hui G, Yu-ying G, Wei-min S, Yong-hua Q and Guang-pu W 2007 *J. Shanghai University* **11** 403

Yongli Y and Shuying C 2008 *J. Semicond.* **29** 2322